ELECTRONIC SUPPLEMENTARY INFORMATION

Liter-scale Production of Uniform Gas Bubbles via Parallelization of Flow Focusing Generators

Heon-Ho Jeong,[a†] Sagar Yadavali,[b] D. Issadore,[b, c,*] and Daeyeon Lee[a,*]

[a]Department of Chemical and Biomolecular Engineering, University of Pennsylvania, Philadelphia, Pennsylvania 19104, USA

[b]Department of Bioengineering, University of Pennsylvania, Philadelphia, Pennsylvania 19104, USA

[c]Electrical and Systems Engineering, School of Engineering and Applied Sciences, University of Pennsylvania, Philadelphia, Pennsylvania 19104, USA

[†]Current address: Department of Chemical and Biomolecular Engineering, Chonnam National University, Yeosu, Jeonnam, Republic of Korea

Movies. Generation of polydisperse gas bubbles, generation of monodisperse liquid droplets, and mass production of gas bubbles in 400-FFG 3D MED-III.

Potential fabrication errors resulting in non-uniform channel dimensions and methods to circumvent such issue. The 3D MED-400 I has a significant non-uniformity in the heights of FFGs. We believe this is due to an error we introduced during spin coating of photoresist. If spin coating of photoresist is performed using a small aliquot of photoresist that is poured in the center region of a silicon wafer (i.e., photoresist only partially covers the wafer instead of the entire area of the wafer), photoresist film that result from such a process has a significant height non-uniformity. Also photoresist around the edges of the wafer tend to have a very different height than the center region of the wafer. Thus, to ensure uniform height over a large area, SU-8 photoresist is poured onto a wafer to ensure full coverage before spin coating is performed. To ensure uniform thickness across the entire wafer, the spin coated photoresist is allowed to stay on a leveled table for 30 min before soft-baking.

3D MED 400-II device suffers from non-uniformity in the width of the channels. We believe the source of this non-uniformity is potentially due to non-uniform UV exposure over the area and/or UV over-exposure. When the exposure time was decreased from 6 to 4 sec, we are able to eliminate such a problem.

Table S1. Physical properties of solution used in experiments

Solution	Surface/Interfacial tension, σ (mNm^{-1})	Viscosity, μ (mPa s)
Nitrogen gas	-	0.018
Pure water	72.0	0.97
2 wt% PVA	47.9	1.59
5 wt% PVA	46.5	3.55
10 wt% PVA	45.9	10.4
Hexadecane (2 wt% Span 80)	5.0 (between oil and water)	4.1

Table S2. Detailed microchannel dimension for 3D MED with 400 parallel FFGs

Fluid Distribution Channel				FFG for dispersed phase			
Channel	Length, l_d (μm)	Width, w_d (μm)	Height, h_d (μm)	Channel	Length, l_f (μm)	Width, w_f (μm)	Height, h_f (μm)
Distribution	600[a]	600	1250	Injection	780	45	25
Supply	3400[b]	1800		Orifice	20	16	
				Outlet	900	65	

[a] and [b] represent the distances between FFGs and distribution channels, respectively.

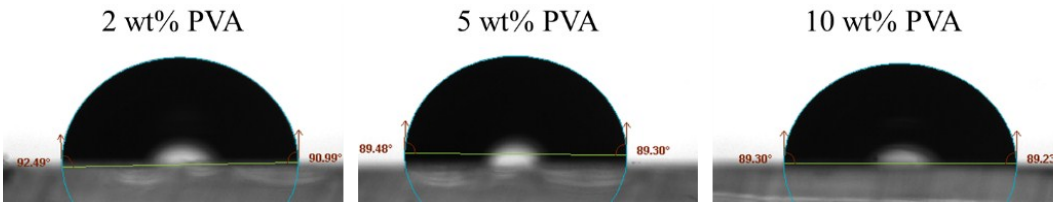

Figure S1. Contact angles of varying PVA concentration on the PDMS substrate.

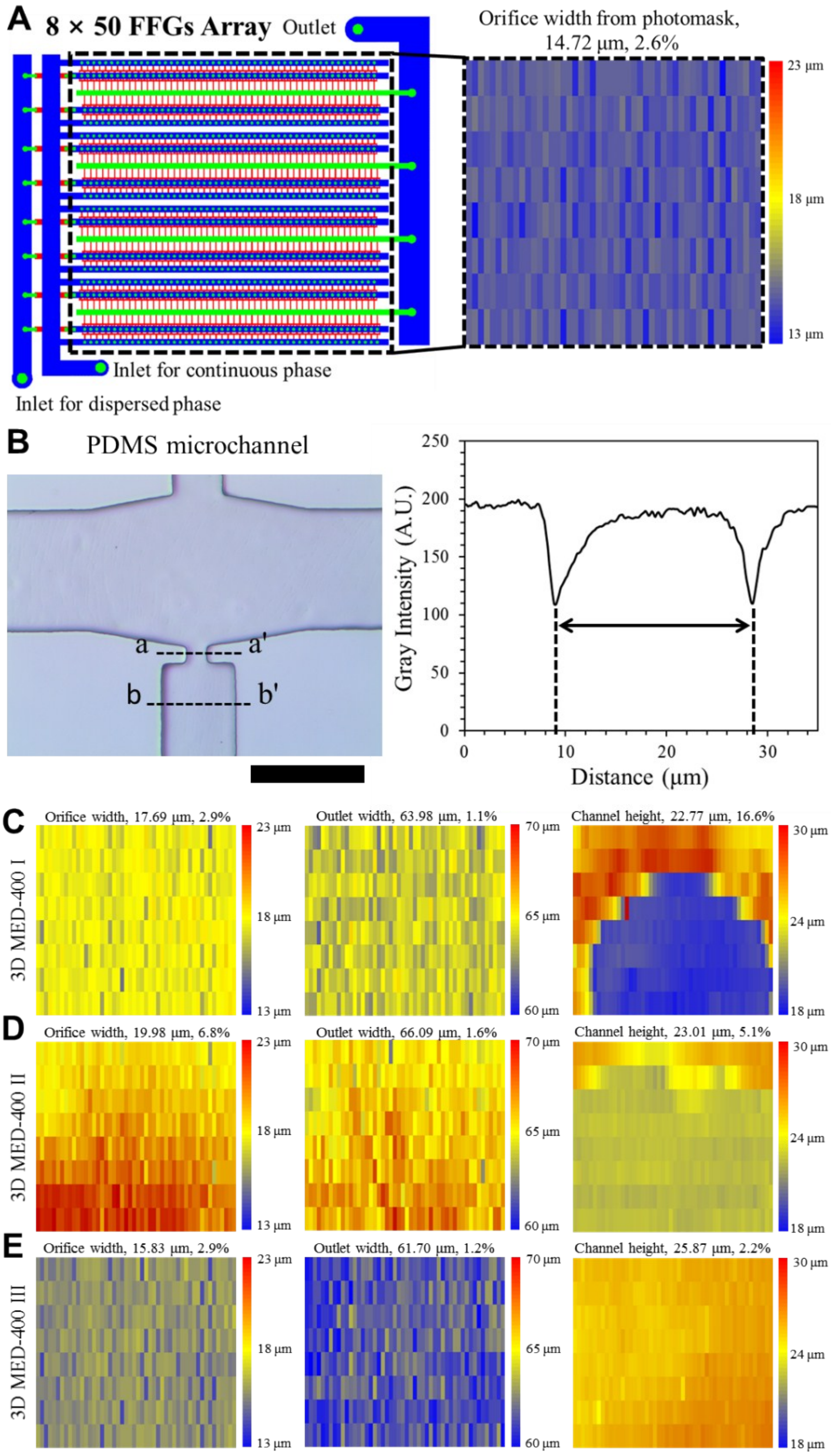

Fig. S2. (A) Heat map showing the orifice width of FFGs in the photomask. (B) Protocol used to measure the microchannel width from an optimal image using line profiling with ImageJ software. Scale bar indicates 100 µm. Heat maps showing the orifice widths, outlet widths and heights of FFGs in 3D MED-400 I (C), II (D) and III (E).

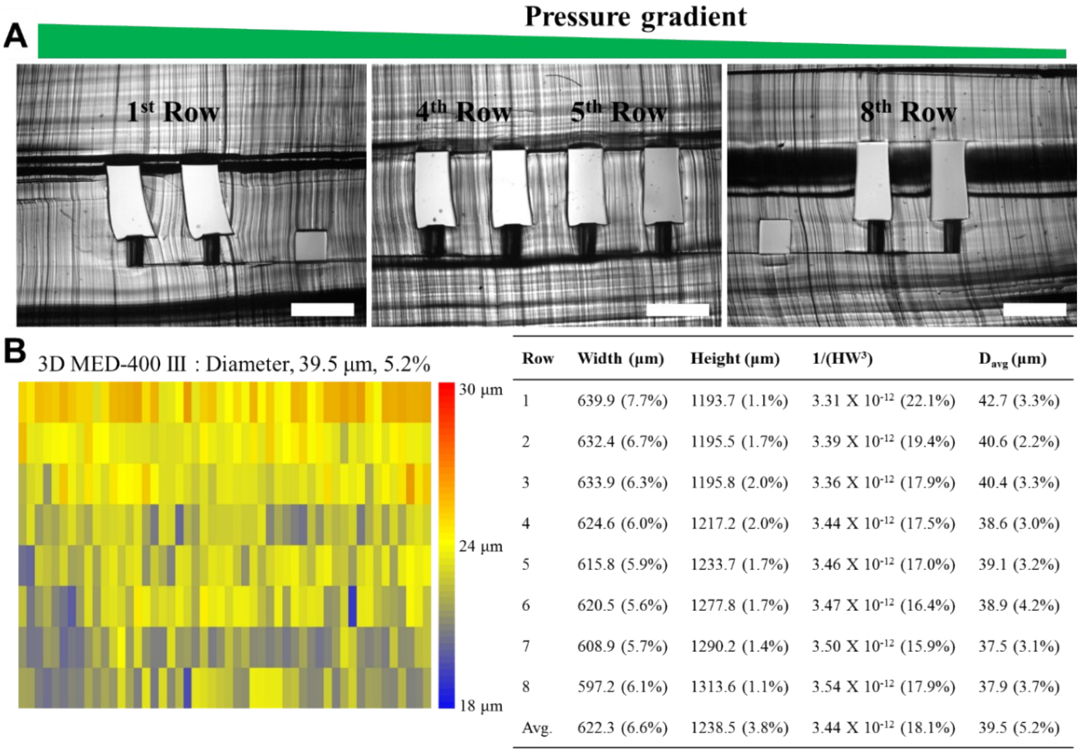

Row	Width (μm)	Height (μm)	1/(HW³)	D_{avg} (μm)
1	639.9 (7.7%)	1193.7 (1.1%)	3.31×10^{-12} (22.1%)	42.7 (3.3%)
2	632.4 (6.7%)	1195.5 (1.7%)	3.39×10^{-12} (19.4%)	40.6 (2.2%)
3	633.9 (6.3%)	1195.8 (2.0%)	3.36×10^{-12} (17.9%)	40.4 (3.3%)
4	624.6 (6.0%)	1217.2 (2.0%)	3.44×10^{-12} (17.5%)	38.6 (3.0%)
5	615.8 (5.9%)	1233.7 (1.7%)	3.46×10^{-12} (17.0%)	39.1 (3.2%)
6	620.5 (5.6%)	1277.8 (1.7%)	3.47×10^{-12} (16.4%)	38.9 (4.2%)
7	608.9 (5.7%)	1290.2 (1.4%)	3.50×10^{-12} (15.9%)	37.5 (3.1%)
8	597.2 (6.1%)	1313.6 (1.1%)	3.54×10^{-12} (17.9%)	37.9 (3.7%)
Avg.	622.3 (6.6%)	1238.5 (3.8%)	3.44×10^{-12} (18.1%)	39.5 (5.2%)

Fig. S3. Non-uniform pressure applied between the soft and hard masters can result in deformation of distribution channels as shown in this Figure. (A) Optical images for representative distribution channel as pressure gradient during double-sided imprinting. High pressure induce the large deformation of distribution channel. Scale bars indicate 1mm. (B) Bubble diameter variation under large variation of distribution channel. The FFG variation is same with 3D MED-400 III as shown in Figure S5E. The heat map shows bubble diameter variation pattern at 39.5 μm average diameter. And a table shows change of average bubble diameter at individual row of distribution channel with gradually increased channel resistance.

Table S3. Pearson correlation coefficient between orifice/outlet resistance and bubble size in 400-FFG 3D MEDs

	Orifice resistance vs. bubble size	Outlet resistance vs. bubble size
400-FFG 3D MED-I	0.51	- 0.46
400-FFG 3D MED-II	0.44	0.51
400-FFG 3D MED-III	- 0.30	- 0.41